

Simulating ice thickness and velocity evolution of Upernavik Isstrøm 1849–2012 by forcing prescribed terminus positions in ISSM

Konstanze Haubner^{1,2}, Jason E. Box¹, Nicole J. Schlegel^{3,4}, Eric Y. Larour³, Mathieu Morlighem⁵, Anne M. Solgaard¹, Kristian K. Kjeldsen⁶, Signe H. Larsen^{1,7}, Eric Rignot^{3,5}, Todd K. Dupont⁸, and Kurt H. Kjær²

¹Geological Survey of Denmark and Greenland (GEUS), Copenhagen, Denmark

²Centre for GeoGenetics, Natural History Museum, University of Copenhagen, Copenhagen, Denmark

³Jet Propulsion Laboratory (JPL), California Institute of Technology, Pasadena, CA, USA

⁴University of California, Los Angeles, CA, USA

⁵Department of Earth System Science, University of California-Irvine, Irvine, CA, USA

⁶DTU Space - National Space Institute, Technical University of Denmark, Department of Geodesy, Kgs. Lyngby, Denmark.

⁷Centre for Ice and Climate, Niels Bohr Institute, University of Copenhagen, Copenhagen, Denmark

⁸Miami University, Oxford, OH, United States

Correspondence to: Konstanze Haubner (khu@geus.dk)

Abstract. Tidewater glacier velocity and mass balance are ~~sensitive to terminus retreat~~ known to be highly responsive to terminus position change. Yet, it remains challenging for ice flow models to reproduce observed ice ~~marginal margin~~ changes. Here, using the Ice Sheet System Model (ISSM; Larour et al., 2012), we simulate the ~~1849–2012~~ ice velocity and thickness changes ~~on of~~ Upernavik Isstrøm ~~using the Ice Sheet System Model (ISSM; Larour et al., 2012)~~, by prescribing observed glacier terminus changes. We find that a realistic ISSM simulation of the past mass balance and velocity evolution of Upernavik Isstrøm is highly dependent on terminus retreat. At the end of the (NW Greenland) by prescribing a collection of 27 observed terminus positions spanning 164 year simulation, the 1990–2012 ice surface elevation and velocities and are within $\pm 20\%$ of the observations. Thus, our model setup provides a realistic simulation of the years (1849–2012) evolution for Upernavik Isstrøm. Increased ice flow acceleration is simulated. The simulation shows increased ice velocity during the 1930s, the late 1970s and between 1995 and 2012, coinciding with increased prescribed when terminus retreat was observed along with negative surface mass balance anomalies and terminus retreat. The simulation suggests three distinct periods of mass change. Three distinct mass balance states are evident in the reconstruction: (1849–1932) having with near zero mass balance, (1932–1992) with ice mass loss dominated by ice dynamical flow, and (1998–2012), where when increased retreat and negative surface mass balance anomalies lead to mass loss twice that of any earlier year. The main products resulting from this study are period. Over the multidecadal simulation, mass loss was dominated by thinning and acceleration responsible for 70 % of the total mass loss induced by prescribed change in terminus position. The remaining 30 % of the total ice mass loss resulted directly from prescribed terminus retreat and decreasing surface mass balance. Although the method can not explain the cause of glacier retreat, it is a reconstruction of ice flow and geometry during 1849–2012 reconstruction of surface elevation, velocity and grounding line position of Upernavik Isstrøm, and can serve as a metric for evaluating simulations investigating the effect of calving laws.

1 Introduction

In recent decades, glaciers terminating into the ocean (tidewater glaciers) ~~show increasing melt rates and have exhibited widespread thinning and velocity~~ acceleration (e.g. Pritchard et al., 2009; Rignot et al., 2011; Velicogna et al., 2014; Khan et al., 2015). Increased air and ocean temperatures induce increased surface melt rates and frontal retreat (Podrasky et al., 2012; Rosenau et al., 2013; Moon et al., 2014), represented by submarine melt and iceberg ~~break-off (calving)~~ calving. The Greenland ice sheet ~~consists of has~~ more than 240 tidewater ~~glaciers~~ glacier outlets (Rignot and Mouginot, 2012) and its mass balance is highly affected by changes in tidewater glacier discharge (van den Broeke et al., 2009; Bevan et al., 2012; McMillan et al., 2016). ~~Global sea level is influenced by Greenland's ice mass changes (e.g. Rignot et al., 2011; Gardner et al., 2013) and sea level have dominated global sea level contributions of the past two decades (e.g. Rignot et al., 2011; Gardner et al., 2013).~~ Sea level projections rely on models to estimate discharge and Greenland's contribution to sea level ~~that are coming more into line with observations (Shepherd and Nowicki, 2017).~~ However, ~~ice flow models still do not fully reproduce observed changes in calving front retreat and ice flow speed (Nick et al. (2009), IPCC, 2013 chapter 13)~~ accurate simulation of terminus position remains a major challenge (Nick et al., 2009, IPCC, 2013 chapter 13).

Tidewater glacier retreat occurs due to calving (Benn et al., 2007; Nick et al., 2010) and submarine ~~frontal~~ melt (Motyka et al., 2011; O'Leary and Christoffersen, 2013; Morlighem et al., 2016a; Rignot et al., 2016). Yet, no universal calving law exists (Benn et al., 2007) and model approaches either (1) focus on the development and performance of a particular calving law (e.g. Cook et al., 2014; Todd and Christoffersen, 2014); (2) ~~simplify the glacier simulation~~ simplify glacier simulations using flow line or flow band models (e.g. Nick et al., 2013; Lea et al., 2014), neglecting e.g. across-flow stresses or (3) ~~are too complex and determine glacier terminus changes on ice particle scale and are thereby~~ not well suited for long-term studies (Åström et al., 2013, 2014).

Upernavik Isstrøm (UI), a set of West Greenland tidewater glaciers, has been the focus of several observational studies. Weidick (1958) compiled historical records of UI terminus positions between 1849 and 1953, concluding that terminus retreat had increased starting in the 1930s. Observed periods of increased UI terminus retreat in 1931 to 1946, in the late 1990s and in 2005–2009 correlate with elevated air temperatures (Andresen et al., 2014). Two ~~dynamic ice loss events~~ periods of increased dynamically driven ice loss took place on UI between 1985–2010 (Kjør et al., 2012) and were responsible for 80 % of the ice mass loss during 1985–2012 (Khan et al., 2013). ~~Hence, previous~~ Previous studies either simulate tidewater glacier retreat with ice flow models or discuss observed terminus changes and its implications for tidewater glaciers. In this study, we combine observations and ice flow models by using observed terminus positions in the Ice Sheet System Model (ISSM; Larour et al., 2012) to simulate Upernavik's glacial system evolution from 1849, near the end of the Little Ice Age, to 2012. We reconstruct the 1849 ice surface elevation and force ISSM glacier terminus retreat with 27 observed terminus positions.

This study does not aim to simulate physically caused retreat, instead we evaluate the effects of changing termini on UI's ice surface elevation and velocity. We (1) investigate whether prescribed terminus change produces a realistic thinning and velocity history; (2) compare simulated mass loss, surface elevation and velocity changes with 1985–2012 observations; and

(3) correlate the calculated dynamic ice loss with observational studies. ISSM produces a monthly-weekly reconstruction of UI ice elevation, grounding-line position, thickness and surface velocity from 1849–2012.

2 Area and Data

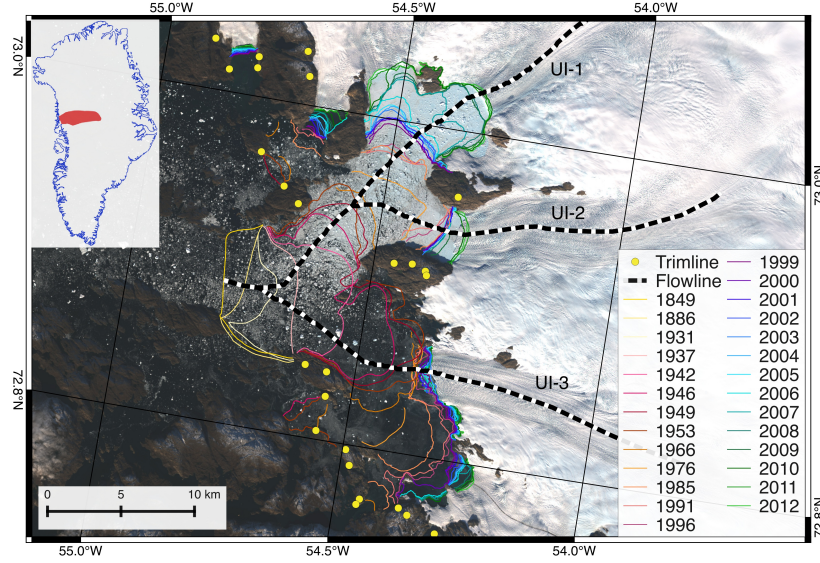


Figure 1. Upernavik Isstrøm’s observed margin front positions between 1849 and 2012 (lines) and trimline positions (yellow dots; Kjeldsen et al., 2015). The background image is from Landsat 8 (September 2013). Inset is the location and shape of the Upernavik catchment (red area), defined-determined by 2008/09 surface velocity from Rignot and Mouginot (2012), which define the model domain.

UI has a catchment area of 64,667~64,700 km², terminating into several tidewater glaciers. We denote-focus on the three main glaciers by-and denote them UI-1, UI-2 and UI-3 from north to south (Fig. 1). Historically, the three glaciers shared the same terminus between 1849 and 1931 (Fig. 1; Weidick (1958))-(Fig. 1; Weidick, 1958). In the 1930s the glaciers separated in two, UI-1/UI-2 and UI-3. UI-1 and UI-2 decoupled after 1966. Historical front positions (Fig. 1) were collected from several sources: 1849–1953 (historical records; Weidick, 1958), 1966–1975 (satellite images; Andresen et al., 2014), 1985–1996 (aerial-photographies (1985) and satellite images; Khan et al., 2013) (aerial photographs (1985) and satellite images; Khan et al., 2013), 1999 to 2012 (satellite images; Jensen et al., 2016).

For initialisation and evaluation of the model we use data from different studies, described in Table 1.

Table 1. Data for ~~initializing~~initialising and evaluating the simulation

Datum	Source	Description
Bed topography	Morlighem et al. (2016b) <u>Morlighem et al. (2015)</u>	Derived with mass conservation approach, extended with bathymetry measurements
Bathymetry measurement		2012 NASA project, led by Eric Rignot and Todd Dupont
Bathymetry measurement	Fenty et al. (2016); OMG Mission. (2016)	NASA project Oceans Melting Greenland OMG
Bathymetry measurement	Andresen et al. (2014)	ship-based <u>Ship-based</u> single point echo sounders
Trim-line <u>Trimline</u> points	Kjeldsen et al. (2015)	Little Ice Age maximum extent (Fig. 1)
Surface mass balance (SMB)	Box (2013)	monthly <u>Monthly</u> data, covering 1840–2012
1985 Digital elevation model (DEM)	Korsgaard et al. (2016)	based <u>Based</u> on aerial photographs, 25 m resolution
2005 DEM	Howat and Eddy (2011)	Greenland Ice Sheet Mapping Project (GIMP), 30 m resolution
2012 DEM	Noh and Howat (2015)	ArcticDEM, 2–10 m resolution
Ice surface velocity	Rignot and Mouginot (2012)	winter <u>Winter</u> 2008/09
Ice surface velocity	Nagler et al. (2017) <u>http://esa-icesheets-greenland.eu/</u> (described in Nagler et al. (2017))	provided <u>Provided</u> by ESA project Climate Change Initiative (CCI) <u>Greenland Ice Sheet</u> in winters between 1991/92 and 2008/09
Ice surface velocity	Howat (2016)	provided <u>Provided</u> by MEaSUREs, in the winters 2000/01, 2007/08 and 2009/10
Ice surface elevation	Thomas and Studinger (2010); Krabill (2010, updated 2016)	from <u>IceBridge</u> ATM; UI-1 in 2009–2012 and UI-3 in 1994, 1999, 2002, 2009, 2010, 2012
Mass change	Wiese et al. (2015); Watkins et al. (2015)	provided <u>Provided</u> by the Jet Propulsion Laboratory (version: JPL RL05M GRACE mascon solution); suitable for regional (300 km scale) ice sheet mass change comparisons (Schlegel et al., 2016)

3 Ice Flow Model

We use the Ice Sheet System Model (ISSM; Larour et al., 2012), a finite-element thermomechanical ice flow model. Ice flow is calculated applying the Shelfy Stream Approximation (SSA; MacAyeal, 1989), ~~using that integrates~~ vertically averaged ice properties (e.g. ~~ice rheology, thickness, velocity)~~ ~~and neglects vertical shear stresses~~. The SSA is well suited for fast-flowing glaciers like Upernavik, where the ice flow is primarily driven by basal sliding. SSA is a 2-D approximation of the 3-D Stokes equation with the ability of upstream ice pushing downstream by including the effects of longitudinal stress and neglecting lateral drag.

Ice viscosity ~~is given by follows~~ Glen’s Flow law (Cuffey and Paterson, 2010), with temperature dependent, spatially varying ice viscosity parameter B , calculated by applying the 1964–1990 UI mean surface air temperature (Box, 2013) to table (Glen, 1955). The initial viscosity is taken from Table 3.4 in Cuffey and Paterson (2010, p. 75). ~~The mean time period is chosen, since surface air temperature and SMB are stable on UI during 1964–1990.~~ The mesh, assuming ice temperature of -5°C and will be refined in section 3.1.

A Coulomb-like friction law is applied on grounded ice:

$$\tau_b = -C^2 N v_b \quad (1)$$

where v_b is the basal velocity, N the effective pressure on the glacier base and C is the friction coefficient (Fig 1, supplementary). Friction is not applied on floating ice.

The model domain is set to the Upernavik catchment, which is defined by the flow direction given by the 2008/09 surface velocity from Rignot and Mouginot (2012) (red area in Fig. 1). We use an adaptive mesh that has a resolution that varies varying between 300–800 m in the area of observed terminus changes and 12 km near the ice divide, resulting in about 17,000 mesh elements. Resolution increases with larger changes in ice velocity (Rignot and Mouginot, 2012) or bedrock topography (Morlighem et al., 2016b) (Morlighem et al., 2017) and decreases stepwise with distance from the front.

The Grounding line position is automatically calculated in each simulation time step (Seroussi et al., 2014). We impose hydrostatic pressure at the terminus and keep the ice velocity and surface elevation constant at the inland boundary, ~~setting ice surface velocity to the 2008/09 observed velocity (Rignot and Mouginot, 2012) and setting ice surface elevation to the GIMP DEM (Howat et al., 2014).~~ No submarine frontal melt or calving rates are applied, since the study aims to simulate ice velocity and thickness changes caused by observational prescribed terminus changes. The ice is allowed to float depending on a hydrostatic criterion (Seroussi et al., 2014).

3.1 Model Initialisation

Since starting the simulation in 1849 extends the present day ice extent by 356 km^2 , model initialisation requires reconstruction of both the ice surface elevation and ice velocities in the extended area. To initialise the model we thus reconstruct the 1849 ice surface elevation and velocity, as described in the following. Over the present day ice covered area, ISSM is initialised with 2008/09 ice surface velocity (Rignot and Mouginot, 2012) and the initial ice surface is given 2005 ice surface elevation

(GIMP; Howat et al., 2014). ~~The present day ice surface velocity is extended to the 1849 ice extent along the flow lines, following fjord bathymetry. Away from the flow lines, missing velocity values are extrapolated.~~ At the 1849 ~~terminus~~marine terminus (given by Weidick, 1958), the ice surface elevation is set to 70 m a.s.l. consistent with marine termini in the area, based on IceBridge data (Krabill, 2010, updated 2016). Trimline data points (Fig. 1; Kjeldsen et al., 2015) mark the 1849 surface elevation and ice extent on the bedrock along the fjords. In the remaining area the ice surface elevation is interpolated. ~~Given the new ice surface and the floatation criterion (Cuffey and Paterson, 2010) :-~~

$$h_{float} = \frac{\rho_{water}}{\rho_{ice}} h_{water},$$

~~with ocean water density $\rho_{water} = 1,023 \text{ kg m}^{-3}$, ice density $\rho_{ice} = 917 \text{ kg m}^{-3}$ and the water depth h_{water} , we calculate the ice shelf floatation height h_{float} . Thus, the ice~~ The ice thickness is set to ~~h_{float}~~ floatation height or to the maximum thickness, defined through the ~~initialized~~ initialised ice surface elevation and bed topography. The ice surface velocity is resolved performing a stress balance solution.

As we are interested in determining how the model geometry and velocity react to the prescribed terminus change and not internal model instability, we relax the model prior to the transient run, bringing ice surface elevation and velocity into equilibrium (following Schlegel et al. (2016)). Equilibrating model geometry and velocity requires constant forcing, i.e. a stable SMB. The SMB at Upernavik is found to be stable in 1854–1900 and 1964–1990. The mean 1854–1900 SMB value is used for equilibrating the model for 1849 conditions and 1964–1990 is set as the SMB reference period to evaluate simulated mass balance.

We perform two ~~successive relaxations to equilibrate the model stepwise, each relaxation starting from previous relaxed model~~

Table 2. Steps for model initialisation

Step	Input	Output
Relaxation 1	GIMP extended to 1849 terminus position, Ice viscosity (initial guess), Basal friction (initial guess)	Reconstructed 1849 ice thickness and velocity
Thermal Inversion	Ice thickness and velocity from relaxation 1 Surface velocity from relaxation 1, Ice viscosity from thermal	Improved ice viscosity Inverted basal friction
Relaxation 2	Ice thickness from relaxation 1, Ice viscosity from thermal, Basal friction from inversion	Steady state ice thickness and velocity

~~applying relaxation runs stepwise (Table 2), keeping SMB constant to the 1854–1900 mean SMB value (Box, 2013).~~ The first relaxation ~~recalculates ice surface elevation and velocity constrained by ice flow equations implemented in ISSM, to minimise inconsistencies between reconstructed ice surface elevation and velocity, resulting from data interpolation onto the mesh and~~

~~extrapolation. The basal friction coefficient for~~ provides reconstructed 1849 ice thickness, given the GIMP surface elevation extended to the 1849 terminus. Thus, in the first relaxation ~~is chosen so that the~~ basal friction is based on the assumption that driving stress is ~~balanced by basal drag equal to basal stress~~ at any given point ~~using the initial geometry~~.

~~The first relaxation is stopped after 125 years simulation and provides ice thickness and velocity for the second relaxation.~~ Given

5 computed ice velocity ~~and thickness~~ from the first relaxation, ~~ice viscosity and~~ basal friction can be redefined. The ~~Basal ice~~ viscosity is calculated by extruding the model with 15 layers and solving for the thermal steady state based on forcing the surface with 1854–1900 UI mean surface air temperature (Box, 2013). The basal friction coefficient is constant in time, but varies in space, and is calculated by an adjoint-based inversion, following Morlighem et al. (2010) and MacAyeal (1993), ~~minimising the error between the observed velocity and the simulated velocity given the updated ice viscosity from the thermal~~
10 ~~steady state simulation~~.

The second relaxation runs for 5,000 years until ice velocity and thickness are equilibrated, ~~provided with ice thickness from the first initialisation, simulated ice viscosity and inverted basal friction~~. The end state of this relaxation provides the initial values of simulated ice ~~thickness, surface velocity and pressure at the bed~~ ~~surface elevation and surface velocity~~ for the 1849–2012 simulations.

15 3.2 Simulation ~~Setup~~~~setup~~

We run two different model simulations: (1) a control run $\text{ISSM}_{\text{control}}$, forced only by monthly SMB (Box, 2013) using a fixed terminus at the observed 1849 ice margin and (2) a prescribed terminus change simulation ISSM_{PT} , forced by monthly SMB and observed calving front positions. $\text{ISSM}_{\text{control}}$ serves to estimate the ice mass, velocity and ~~surface elevation~~ ~~thickness~~ changes that are simulated without prescribed terminus change.

20 The prescribed terminus position change in ISSM_{PT} is implemented through a ~~levelset-based~~ ~~levelset-based~~ method (Bondzio et al., 2016, 2017) and performed in July of the observation year, according to observed terminus positions (Fig. 1). The highest surface air temperatures and melt rates on UI are observed in July, increasing the likelihood of terminus retreat (van As et al., 2016). We introduce 20 additional calving front positions, ~~linearly interpolated created through linear interpolation~~ between the observed termini ~~positions~~ and constrained by the mesh resolution ~~to reduce induced~~. ~~The additional calving fronts aim to~~
25 ~~improve realistic simulation behavior by splitting large~~ ice area changes ~~that are causing numerical instabilities in the ice flow equations~~ ~~induced by the prescribed terminus changes into smaller areas within shorter time periods~~.

~~Within the prescribed ice area, the grounding line is evolving freely and floating tongue formation is thereby allowed.~~

The simulation evaluation time step is set to 73 h, constrained by the CFL condition (Courant et al., 1967), ensuring the numerical stability solving the ice flow equations at each time step.

30 4 Results and ~~Comparison~~~~comparison~~

During the simulation, most of the ice ~~surface elevation~~ ~~thickness~~ and velocity changes occur near the central flow lines of UI-1, UI-2 and UI-3. ~~Elevation and velocity changes~~ ~~Simulated changes in ice thickness and velocity~~ in the majority of the

model domain (more than 70 km inland from the 2012 terminus or 5 km away form-from the central flow lines of the three glaciers) are below 25 %, corresponding to below changes of 20 m and 10 m y⁻¹ changes over 164 simulation years. Hence, in the following we present relative and absolute changes in ice velocity and surface-elevation-thickness along the central flow lines of UI-1, UI-2 and UI-3 (from the 2012 terminus reaching 30 km upstream ~~÷~~ (Fig. 1).

5 4.1 Model comparison

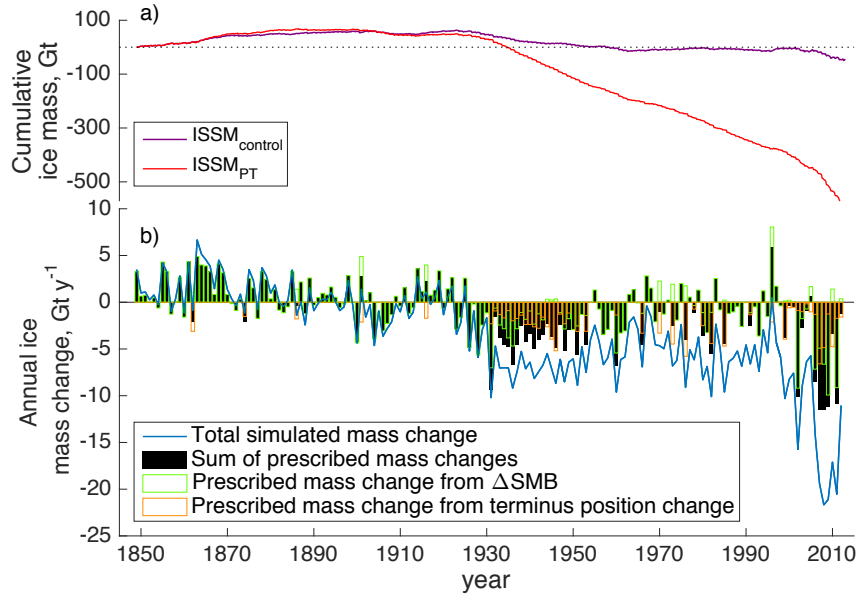


Figure 2. a) Simulated cumulative ice mass in Gt. ISSM_{PT} changes are shown in red; control run changes in purple. b) The blue curve illustrates simulated annual change in ice loss-mass for ISSM_{PT}. The black bars indicate the ice mass that is removed due to ΔSMB and prescribed change-changes of the terminus position. The green outline marks the portion of mass change due to ΔSMB, and the orange outline the share of prescribed terminus change respectively.

Between 1849 and 2012, ISSM_{control} shows less than 7 % surface-elevation-lowering-and-thinning and 5 % acceleration, simulating a change in velocity less than 120 m y⁻¹ and a surface-elevation-lowering less than 10thinning less than 30 m along the central flow lines for the entire period. In contrast, ISSM_{PT} produces on-average-36a thinning between 20 % elevation-lowering in-1849–2012, reaching up to 84along the flow lines and up to 60 % at-the-in the area between 2012UI-2-terminus-terminus and 70 km upstream in 1849–2012, corresponding to thinning between 100 and 450 m along the flow lines. The average ice surface velocity increase along UI-1 and UI-2 is 180 % and on-UI-3-is-47 % on UI-3. Cumulative ice mass loss over the simulation period of the entire model domain (converted from modelled water equivalent assuming 917 kg m⁻³ ice density) was by the end of the model simulation –4550 Gt for ISSM_{control} and –585 Gt for ISSM_{PT} (Fig. 2). The following section focuses on presenting-99 % of simulated ISSM_{control} mass loss was prescribed by ΔSMB while 30 % of total ice mass loss simulated by

ISSM_{PT} was prescribed, with ΔSMB accounting for 9 % (−50 Gt) and prescribed terminus position change contributed 21 % (−121 Gt). Thus, 70 % of by ISSM_{PT} simulated mass loss is caused by thinning and acceleration. The succeeding subsections describe ISSM_{PT} results in more detail.

5 4.2 Mass balance

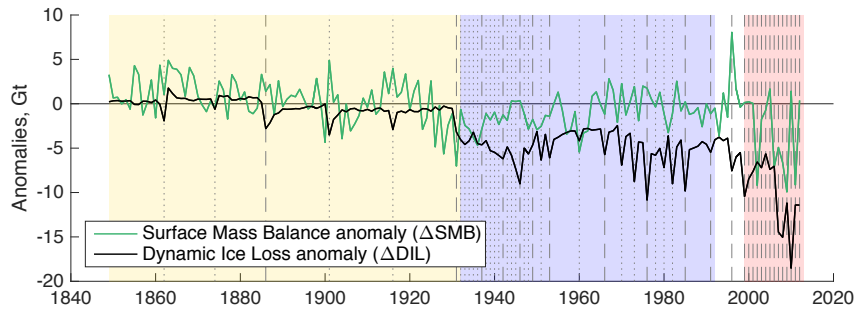


Figure 3. Simulated ice mass changes from anomalies (relative to 1964–1990 mean values) for the simulation ISSM_{PT}. The background is highlighted in yellow for periods of time where ΔSMB controlled MB, blue is where ice mass loss is driven by ΔSMB and ΔDIL and red, where ΔSMB and ΔDIL have equally increased influence on the MB. Prescribed termini changes are marked with dashed (observations) and dotted (interpolation) lines.

In the following section we focus on the simulated mass balance (MB) through the model runs (see cumulated mass change in Fig. 2). For tidewater-marine terminating glaciers, mass balance can be attributed to either changes in SMB or changes in dynamic ice loss (DIL). A tidewater glacier is in equilibrium, when SMB and DIL are in balance. Deviations in SMB and DIL change the glacier and its stability, hereafter referred to as anomalies ΔSMB and ΔDIL . SMB is a model input and ΔSMB are calculated relative to the mean value of the stable UI period 1964–1990 SMB. ΔDIL is calculated as the residual between the simulated MB and ΔSMB .

The simulated annual MB for the UI catchment (Fig. 2) is positive from 1849 to 1920. In this period, the MB from the ISSM_{PT} and ISSM_{control} are similar due to very few and small terminus changes (Fig. 2) and MB is thus dominated by ΔSMB . Anomalies in DIL (Fig. 3) are evident by small (−0.5 to −4 Gt) peaks that coincide with prescribed terminus retreat. After 1920, the MB becomes negative, except in 1996, when ΔSMB has a peak (8 Gt), which is attributed to a high winter accumulation (McConnell et al., 2001; Box et al., 2006). Figure 3 highlights three periods in MB trends: (1) 1849–1932, when MB is close to zero near equilibrium, (2) from 1932 to 1992, when the negative total-MB is driven by ΔDIL , and (3) 1998–2012, when SMB and DIL both have high negative anomalies and the total mass loss each year is was twice as high as any year before.

Simulated Khan et al. (2013) and Larsen et al. (2016) measure surface elevation changes from aerial photographs, satellites and digital elevation models between 1985 and 2010. These yield a total mass change during different time periods and congruent to our calculations ΔDIL is estimated as the residual of mass change and ΔSMB . Both studies refer to different areas

Table 3. Observed vs. simulated ice mass changes (with ISSM_{PT}).

	Khan et al. (2013) ^a		Larsen et al. (2016)		
	1985 – 2002/05	2002/05 – 2010	2000 – 2005	2006 – 2008	2009 – 2011
Observed <u>Total observed ice mass</u> changes, Gt	-32 ± 9	-17 ± 10	-6 ± 20	-25 ± 14	-39 ± 17
Simulated <u>Total simulated ice mass</u> changes, Gt	-37^b	-32^b	-48	-41	-44
<u>Observed dynamic ice loss</u> , Gt	29 ± 9	12 ± 11	5 ± 10	16 ± 4	27 ± 4
<u>Simulated dynamic ice loss</u> , Gt	32^b	26^b	40	24	28

^a converted from km³ to Gt ice equivalent

^b results from 2002/05 as mean values of that time

within the UI catchment. Table 3 presents a comparison of the observed mass changes and our simulation results, recalculated for the particular areas. Due to sparse data coverage Khan et al. (2013) combine surface elevation measurements acquired between 2002 and 2005 to quantify elevation changes and refer to this period as 2002/2005. The average of simulated ice mass loss between 2002 and 2005 is taken for comparison with the 2002/2005 observations from Khan et al. (2013).

- 5 ~~Simulated total ice~~ mass changes in 1985–2002/05 and 2009–2011 2005 and 2006–2011 correspond with observed ice mass changes from Kjaer et al. (2012); Khan et al. (2013) Khan et al. (2013) and Larsen et al. (2016) (Table 3). ~~In 2002/05–2010 and 2000–2005, simulated mass changes are 85% larger than the maximum of what is observed. DIL is 85% the mass change from 1985–2010. During~~ Additionally, the DIL during 2000 to 2005 ~~DIL is 85%~~ makes up 83 % of the mass change and in 2006–2011 ~~the DIL is 60%~~ this percentage is reduced to 64 % of mass changes, in agreement with Khan et al. (2013) and Larsen et al. (2016).
- 10 ~~In 2000–2005, however, simulated total mass changes are 81 % larger than the maximum of what is observed.~~

A comparison with GRACE, that measures gravity field variations from which mass change is computed, shows equivalent seasonal mass loss fluctuations in summer and mass gain in winter with an overall negative trend. The simulated mass change rates resemble 98 % of GRACE's rate (see supplementary).

4.3 Ice ~~surface elevation~~ thickness

- 15 ISSM_{PT} simulates ~~20–100~~ 10–80 % ~~ice surface lowering thinning~~ from 1849 to 2012 over an area reaching ~~50~~ 70 km upstream from the 2012 terminus (see supplementary). Transient surface elevation changes along the central flow lines of UI-1, UI-2 and UI-3 are visualised in movie01 (supplementary). The model simulation shows increased surface lowering in the time periods 1930/40, 1970/80 and from 2000 onwards.

- ~~Simulated surface elevation in~~ To evaluate simulated ice thickness, we compare simulation results with the residual ice thickness obtained from observed surface elevation data and the bed topography from Morlighem et al. (2017), that is used in the simulation setup. We refer to the supplementary for illustrations of spatial comparisons between simulation results and observations. Simulated thickness in 2005 lies within ± 20 30 % of ~~the observed surface elevation~~ observed thickness (GIMP) ~~and in 2012 it lies within –20 and –10,~~ except in the shear margin regions of UI-1, where simulated ice thickness is
- 20

too high by up to 160 % of observations. A comparison of absolute ice thickness in 2005 shows up to 200 m lower simulated thickness than observed, apart from the shear zones of UI-1, where the ice is up to 200 m thicker than observed. Differences between the simulated 2012 ice thickness and observations (ArcticDEM) show the same pattern with less difference in the UI-1 shear zone. The 1985 DEM based on aerial photographs (Korsgaard et al., 2016) reaches covers only the UI coastal area, reaching at most 40 km inland. Simulated surface elevation is 60 and covering primarily the UI-3 area. Simulated ice is 20 to 100 % higher thicker around UI-1 and UI-2 than the 1985 reconstruction observations and 10 % lower thinner on average along UI-3.

NASA Operation IceBridge (Thomas and Studinger, 2010; Krabill, 2010, updated 2016) provides ice surface elevation along UI-1 (2009–2012) and UI-3 (1994, 1999, 2002, 2009, 2010, 2012). A mean value comparison along the UI-3 flow lines line illustrates that the simulated ice thickness is on average 10 % less than observations (Fig. 4), illustrate that the simulated surface elevation is two third of that observed 0–5. The same comparison on UI-1 shows simulated ice thickness being 104 km upstream of the 2012 terminus and 56–62 % of observations close to the UI-1 terminus and 93 % of that observed 5–10 km upstream of the 2012 terminus. Simulated surface elevations close to the UI-1 terminus resemble IceBridge observations to 90–100%. Further upstream, UI-1 simulation results are 70–80% of observed ice surface elevation. terminus.

Observed IceBridge and simulated surface elevation along flow lines 5 km downstream and 20 km upstream of the 2012 terminus have high correlation with R-squared values of 0.93–0.80 for UI-1 and 0.97–0.95 for UI-3.

ISSM_{PT} simulates trends in elevation that are equivalent to those of the major thinning trends as described by Kjaer et al.

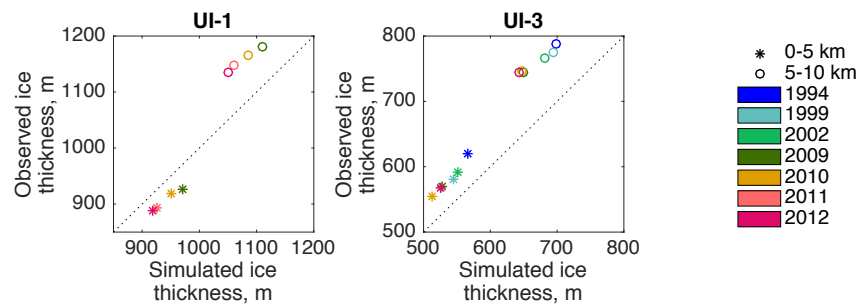


Figure 4. Observed vs. simulated ice surface elevation thickness along flight lines (IceBridge surface elevation data; Thomas and Studinger, 2010; Krabill, 2010, updated 2016) over UI-1 and UI-3. Stars mark mean values between 0 and 5 km from the 2012 terminus, dots refer to mean values 5–10 km upstream. Flight lines over UI-1 are available for the years 2009, 2010, 2011, 2012 and over UI-3 in the years 1994, 1999, 2002, 2009, 2010, 2012.

(2012) and Khan et al. (2013) between 1985 and 2010 on UI-1 and UI-3, though not on UI-2. Note that the observed thinning south of UI-3 between 1985 and 1991 (Khan et al., 2013) is not reproduced in ISSM_{PT}.

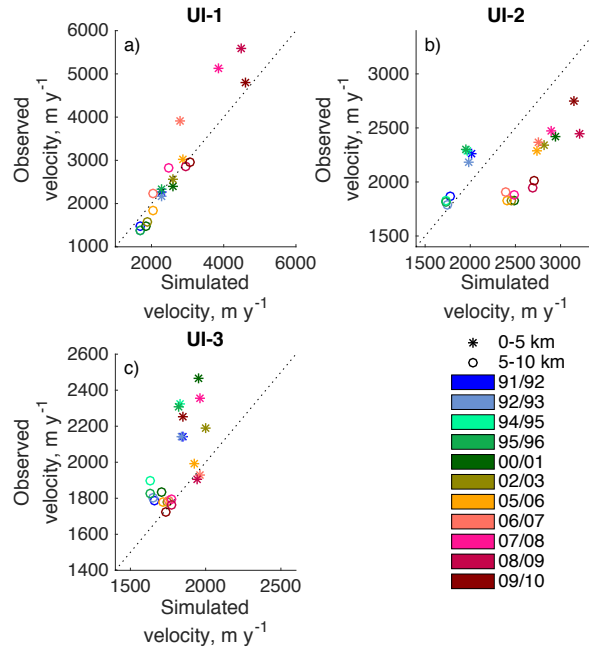


Figure 5. Observed vs. simulated ice surface ~~velocities-velocity~~ along the central flow lines of UI-1, UI-2 and UI-3. Stars mark mean ~~velocities-velocity~~ between 0 and 5 km from the 2012 terminus, dots refer to mean values 5–10 km upstream. ~~Velocity data in the winters of Winter velocity maps for~~ 1991/92, 1992/93, 1994/95, ~~1995/96~~, 2002/03, 2005/06, ~~2006/07~~ and 2008/09 are ~~provided by CCI (Nagler et al., 2017)~~ produced from data available from <http://esa-icesheets-greenland-cci.org/> and described in Nagler et al. (2017). Winter velocity maps from 2000/01, 2007/08 and 2009/10 are given by MEaSUREs (Howat, 2016).

4.4 Ice surface velocity

By the end of the ISSM_{PT} simulation, ice flow ~~velocities-doubles-velocity has doubled~~ at UI-1 and UI-2 and ~~accelerates~~ increased by 55 % at UI-3 compared to 1849. The simulated ice surface velocity evolution in plane view over the study period can be viewed in movie02 (supplementary). Short-term accelerations coincide with the induced ice mass change due to the prescribed terminus change (see movie01, supplementary). The simulation reproduces seasonal and annual velocity variations due to the SMB forcing in the model. Small (20 m y^{-1}) annual velocity fluctuations are forced by seasonal SMB fluctuations. Each retreat from the prescribed terminus change is followed by ~~an~~-acceleration between 1 and 70 % and 5–30 % surface lowering, lasting 0.5 to 6 months.

Simulated 2009 ice surface velocity is within $\pm 20 \%$ of observations from Rignot and Mouginot (2012), except in the shear margins, where simulated velocities are up to ~~200250 % of higher than~~ observations. Winter velocity maps between 1991 and 2010 (Table 1) are used to evaluate recent changes in simulated velocity. Observed and simulated winter ice surface velocity averaged between 0 and 5 km and 5 to 10 km upstream of 2012 terminus (Fig. 5) have R-squared values of 0.90 on UI-1, 0.88

on UI-2 and 0.92 on UI-3. Observations show 20 % velocity increase on UI-1 from 07/08 to 08/09, however, this is not captured in ISSM_{PT}.

5 Discussion

The comparison of ISSM_{PT} and ISSM_{control} shows that the ice surface velocity and elevation thickness are significantly affected by the prescribed marginal changes. After each prescribed terminus change, ISSM_{PT} simulates short (0.5 to 6 months) periods of faster flow (1–70 % acceleration), and the surface elevation lowers up to 30 % at the new terminus in response to the ice flow acceleration. These are dynamic readjustments to the instantly reduced terminal flow resistance from the prescribed retreat, which is induced in discrete time steps.

While ISSM_{PT} produces maximum velocity and surface elevation changes of 275 % and 84 % respectively over the simulation period, ISSM_{control} simulates minor changes (maximum ± 7 %) in ice ~~velocity and surface elevation, describing only changes in thickness and velocity, representing sole mass changes prescribed by Δ SMB~~. This highlights the importance of simulated terminus retreat in order to reproduce a UI glacial system evolution. In 1985–2012, ISSM_{PT} simulates mass changes similar to observations (Kjær et al., 2012; Khan et al., 2013; Larsen et al., 2016) ~~and ice surface elevation being within 20% of GIMP or ArcticDEM and CCI or MEaSUREs velocity observations~~.

Recent studies suggest dividing mass balance into atmospheric and dynamically driven processes (Nick et al., 2009; Howat and Eddy, 2011; Kjær et al., 2012; Enderlin and Howat, 2013). Our simulation indicates three distinct MB periods when considering Δ SMB and Δ DIL. From the simulation start in 1849 to 1932, the total UI MB is the same for ISSM_{control} and ISSM_{PT}, only diverging five times by one to four Gt y^{-1} when prescribed retreat is enforced. The increasing Δ SMB trend leads to a positive MB and thus mass gain. ISSM_{PT} ~~velocities start~~ velocity starts to differ from ISSM_{control} following the first prescribed retreat in 1862, showing a short (< 1 month) acceleration. The simulation indicates stable glacier behaviour without dynamically caused acceleration or thinning.

From 1925 onwards, Δ SMB reveals a negative trend, initiating the negative MB trend that lasts until the simulation end in 2012. Between 1931 and 1992, in two instances (1931–1960 and 1960–1992), 5–7 year periods of sustained less-positive SMB are followed by approximately 20 year long periods of elevated Δ DIL.

Within ~~this~~ these 60 years of simulation 31 terminus changes are prescribed, each removing 0.4–5 Gt of ice, which is as much as each of the five terminus changes the preceding 82 years (Fig. 2). The simulated mass loss in this period is therefore highly controlled by the prescribed retreat. Δ DIL consists of the removed ice mass at a prescribed retreat and of changes in ice mass flux caused by the acceleration of the glacier. We simulate two increased Δ DIL periods preceded by low Δ SMB as the result of observed terminus retreat. Induced by the prescribed terminus change in 1960 and 1966, a new period with increased Δ DIL lasts until 1992. ~~UI's glaciers aim again for equilibrium, interrupted by seven prescribed terminus changes.~~

From 1999 onwards, Δ DIL and Δ SMB are roughly equivalent in contribution to the elevated negative MB. The simulation computes elevated dynamic ice loss due to 5.5 km terminus retreat on UI-1 within 12 years. We can not resolve, whether the increased retreat of UI-1 is due to (1) the change in Δ SMB from positive to negative values (+7 Gt to -7 Gt) or whether the

glacier itself reaches an unstable position. However, as a result the retreat causes increased simulated Δ DIL adding up to the same amount as the increased negative Δ SMB. UI-2 shows similar behaviour. The result is a negative MB twice as negative as in any year before. In contrast, UI-3 is nearly stable, retreating ~~0.53~0.5~~ km between 1999 and 2012 and even advances in some years. It cannot be determined, whether UI-1 and UI-2 also will reach a stable position soon or whether they will continue to

retreat and accelerate.
~~The simulation reproduces not only the retreat, but also the observed terminus advances~~ Although we primarily discuss prescribed ice margin retreat, it is worth mentioning that our method also includes advancing observed terminus position changes at UI-1 and UI-2 in summer 2012 and at UI-3 in the summers 2001, 2003 and 2007. However,-

MEaSUREs data indicate 20 % speed-up on UI-1 from 2007–2008 to 2008–2009, when a large floating ice tongue breaks off (Larsen et al., 2016). ~~The~~ Yet, the observed acceleration is not captured by the simulation and may be related to unresolved loss ~~in of~~ buttressing in the simulation.

6 Conclusions

Our study shows that ~~glacier front changes are necessary for ice model simulations to reach realistic present day ice surface velocity and elevation. Prescribed~~ prescribing glacier front positions and surface mass balance are necessary to realistically simulate the multidecadal evolution of ice velocity and thickness at Upernavik Isstrøm. Our simulation suggests that dynamic response caused by prescribed terminus position change avoids calving and melt rate estimations and reduces simulated retreat uncertainty. Dynamic ice discharge is responsible for ~~80~~70 % mass change in the 1985–2005 period and thereby plays of the total simulated mass change. Thus, moving terminus positions play an important role for UI's acceleration and thinning. ISSM_{PT} captures The simulation with prescribed terminus changes reproduces distinct mass loss periods of dynamically driven ice mass loss and extends the periods discussed in Kjær et al. (2012) and Khan et al. (2013) from 1985 to 1932. The method is applicable to different glaciers and time periods, since we realistically reconstruct the 164 year UI glacial evolution matching observed velocity, surface elevation and mass changes within $\pm 20\%$ of observations, without any further assumptions.-

Our approach is limited, since it needs defined terminus position changes throughout the simulation period, and it cannot be used Prescribed terminus position change avoids calving and melt rate estimations and reduces simulated retreat uncertainty. Yet, our approach requires knowledge about terminus positions and thus cannot be applied in future projections. However, the simulation results show the importance of including calving into ice sheet models calving in order to capture produce velocity and thickness changes of a glacier change of tidewater glaciers. Better physically based calving laws are needed to understand and predict future glacier behaviour and glacier contribution to sea level rise. Our method can help The method of prescribed terminus change is a useful tool evaluating calving laws during past simulations before applying them in or determining calving law parameters for hindcast simulations before they are applied to future simulations. Short-term simulations with prescribed terminus position change might help answer the question, changes can determine what observations are needed to evaluate and construct new calving laws, by establishing if seasonal terminus position variations are necessary to capture

long-term glacier behaviour, ~~to determine what data is needed to evaluate and construct new calving laws~~. Future work could include comparisons with ~~the simulations using~~ physically based calving laws (e.g. Bondzio et al., 2016; Morlighem et al., 2016a) ~~and as well as the~~ application of our method to other tidewater glaciers.

5 *Author contributions.* KH, NJS, EYL, JEB, KHK, KKK and SHL designed the study and setup the model. KH performed the study and data comparison and led the writing of the manuscript, in which she received input and feedback from all authors. MM created the bed geometry from bathymetry data, supported with data from ER and TKD. KKK provided trimline data and observed terminus positions. AMS processed winter ice surface velocity maps from ESA, CCI Greenland.

Competing interests. The authors declare that they have no conflict of interest.

10 *Acknowledgements.* The manuscript improved substantially from the reviewers, and the authors would like to thank Jeremy Bassis and the anonymous reviewer for their constructive comments. This study is part of the project "Multi-millennial ice volume changes of the Greenland Ice Sheet" funded by the Geocenter Denmark. KKK was supported by the Danish Council for Independent Research (~~DF~~
~~4090-00151~~DF-4090-00151). We thank Brian Vinter and his team at Niels Bohr Institute, Copenhagen University, for generously supplying high performance computing resources. We ~~acknowledge the use of bathymetry data provided by Eric Rignot and Todd Dupont, Department~~
15 ~~of Earth System Science, University of California-Irvine, USA, produced during a 2012 NASA campaign. The authors~~ wish to thank Camilla Snowman Andresen, Geological Survey of Greenland and Denmark, for providing bathymetry measurements. Observed termini between 1999 and 2012 were ~~provided by Trine~~ digitized by Trine S. Jensen and Karina Hansen, Geological Survey of Greenland and Denmark. We acknowledge and thank the Ice Sheet System Model group for producing and making available their model. We also acknowledge the use of the DEMs from GIMP, ArcticDEM and Niels Korsgaard and the velocity data provided by ESA (CCI Greenland) and NASA, all available
20 online.

References

- Åström, J. A., Riikilä, T. I., Tallinen, T., Zwinger, T., Benn, D., Moore, J. C., and Timonen, J.: A particle based simulation model for glacier dynamics, *The Cryosphere*, 7, 1591–1602, doi:10.5194/tc-7-1591-2013, 2013.
- Åström, J. A., Vallot, D., Schäfer, M., Welty, E. Z., O’Neel, S., Bartholomäus, T. C., Liu, Y., Riikilä, T. I., Zwinger, T., Timonen, J., and Moore, J. C.: Termini of calving glaciers as self-organized critical systems, *Nature Geoscience*, 7, 874–878, doi:10.1038/ngeo2290, 2014.
- Andresen, C. S., Kjeldsen, K. K., Harden, B., Nørgaard-Pedersen, N., and Kjær, K. H.: Outlet glacier dynamics and bathymetry at Upernavik Isstrøm and Upernavik Isfjord, North-West Greenland, *Geological Survey of Denmark and Greenland Bulletin*, pp. 79–81, doi:10.5194/tc-10-1965-2016, 2014.
- Benn, D. I., Warren, C. R., and Mottram, R. H.: Calving processes and the dynamics of calving glaciers, *Earth Science Reviews*, 82, 143–179, doi:10.1016/j.earscirev.2007.02.002, 2007.
- Bevan, S. L., Luckman, A., and Murray, T.: Glacier dynamics over the last quarter of a century at Helheim, Kangerdlugssuaq and 14 other major Greenland outlet glaciers, *Cryosphere*, 6, 923–937, doi:10.5194/tc-6-923-2012, <http://www.the-cryosphere.net/6/923/2012/>, 2012.
- Bondzio, J. H., Seroussi, H., Morlighem, M., Kleiner, T., Rückamp, M., Humbert, A., and Larour, E. Y.: Modelling calving front dynamics using a level-set method: application to Jakobshavn Isbræ, West Greenland, *The Cryosphere*, 10, 497–510, doi:10.5194/tc-10-497-2016, 2016.
- Bondzio, J. H., Morlighem, M., Seroussi, H., Kleiner, T., Rückamp, M., Mouginot, J., Moon, T., Larour, E. Y., and Humbert, A.: The mechanisms behind Jakobshavn Isbræ’s acceleration and mass loss: a 3D thermomechanical model study, *Geophysical Research Letters*, doi:10.1002/2017GL073309, 2017.
- Box, J. E.: Greenland ice sheet mass balance reconstruction. Part II: Surface mass balance (1840-2010), *Journal of Climate*, 26, doi:10.1175/JCLI-D-12-00518.1, 2013.
- Box, J. E., Bromwich, D. H., Veenhuis, B. A., Bai, L.-S., Stroeve, J. C., Rogers, J. C., Steffen, K., Haran, T., and Wang, S.-H.: Greenland Ice Sheet Surface Mass Balance Variability (1988–2004) from Calibrated Polar MM5 Output*, *Journal of Climate*, 19, 2783, doi:10.1175/JCLI3738.1, 2006.
- Cook, S., Rutt, I. C., Murray, T., Luckman, A., Zwinger, T., Selmes, N., Goldsack, A., and James, T. D.: Modelling environmental influences on calving at Helheim Glacier in eastern Greenland, *The Cryosphere*, 8, 827–841, doi:10.5194/tc-8-827-2014, 2014.
- Courant, R., Friedrichs, K., and Lewy, H.: On the Partial Difference Equations of Mathematical Physics, *IBM J. Res. Dev.*, 11, 215–234, doi:10.1147/rd.112.0215, <http://dx.doi.org/10.1147/rd.112.0215>, 1967.
- Cuffey, K. and Paterson, W.: *The Physics of Glaciers*, Elsevier Science, 2010.
- Enderlin, E. M. and Howat, I. M.: Submarine melt rate estimates for floating termini of Greenland outlet glaciers (2000–2010), *Journal of Glaciology*, 59, 67–75, doi:10.3189/2013JoG12J049, 2013.
- Fenty, A., Willis, J. K., Khazendar, A., Dinardo, S., Forsberg, R., Fukumori, I., Holland, D., Jakobsson, M., Moller, D., Morison, J., Münchow, A., Rignot, E., Schodlok, M., Thompson, A. F., Tinto, K., Rutherford, M., and Trenholm, N.: Oceans Melting Greenland: Early Results from NASA’s Ocean-Ice Mission in Greenland, *Oceanography*, 29, doi:10.5670/oceanog.2016.100, 2016.
- Gardner, A. S., Moholdt, G., Cogley, J. G., Wouters, B., Arendt, A. A., Wahr, J., Berthier, E., Hock, R., Pfeffer, W. T., Kaser, G., Ligtenberg, S. R. M., Bolch, T., Sharp, M. J., Hagen, J. O., van den Broeke, M. R., and Paul, F.: A Reconciled Estimate of Glacier Contributions to Sea Level Rise: 2003 to 2009, *Science*, 340, 852–857, doi:10.1126/science.1234532, 2013.

- Glen, J. W.: The creep of polycrystalline ice, *Proceedings of the Royal Society of London A: Mathematical, Physical and Engineering Sciences*, 228, 519–538, doi:10.1098/rspa.1955.0066, 1955.
- Howat, I. M.: MEaSURES Greenland Ice Velocity: Selected Glacier Site Velocity Maps from Optical Images, Version 2, doi:10.5067/EYV1IP7MUNSV, accessed: 2016-03-27, 2016.
- 5 Howat, I. M. and Eddy, A.: Multi-decadal retreat of Greenland's marine-terminating glaciers, *Journal of Glaciology*, 57, 389–396, doi:10.3189/002214311796905631, 2011.
- Howat, I. M., Negrete, A., and Smith, B. E.: The Greenland Ice Mapping Project (GIMP) land classification and surface elevation data sets, *The Cryosphere*, 8, 1509–1518, doi:10.5194/tc-8-1509-2014, 2014.
- Jensen, T. S., Box, J. E., and Hvidberg, C. S.: A sensitivity study of annual area change for Greenland ice sheet marine terminating outlet
10 glaciers: 1999–2013, *Journal of Glaciology*, 62, 72–81, doi:10.1017/jog.2016.12, 2016.
- Khan, S. A., Kjær, K. H., Korsgaard, N. J., Wahr, J., Joughin, I. R., Timm, L. H., Bamber, J. L., Broeke, M. R., Stearns, L. A., Hamilton, G. S., Csatho, B. M., Nielsen, K., Hurkmans, R., and Babonis, G.: Recurring dynamically induced thinning during 1985 to 2010 on Upernavik Isstrøm, West Greenland, *Journal of Geophysical Research (Earth Surface)*, 118, 111–121, doi:10.1029/2012JF002481, 2013.
- Khan, S. A., Aschwanden, A., Bjørk, A. A., Wahr, J., Kjeldsen, K. K., and Kjær, K. H.: Greenland ice sheet mass balance: a review, *Reports
15 on Progress in Physics*, 78, 046801, doi:10.1088/0034-4885/78/4/046801, 2015.
- Kjær, K. H., Khan, S. A., Korsgaard, N. J., Wahr, J., Bamber, J. L., Hurkmans, R., van den Broeke, M., Timm, L. H., Kjeldsen, K. K., Bjørk, A. A., Larsen, N. K., Jørgensen, L. T., Færch-Jensen, A., and Willerslev, E.: Aerial Photographs Reveal Late-20th-Century Dynamic Ice Loss in Northwestern Greenland, *Science*, 337, 569, doi:10.1126/science.1220614, 2012.
- Kjeldsen, K. K., Korsgaard, N. J., Bjørk, A. A., Khan, S. A., Box, J. E., Funder, S., Larsen, N. K., Bamber, J. L., Colgan, W., van den
20 Broeke, M., Siggaard-Andersen, M.-L., Nuth, C., Schomacker, A., Andresen, C. S., Willerslev, E., and Kjær, K. H.: Spatial and temporal distribution of mass loss from the Greenland Ice Sheet since AD 1900, *nature*, 528, 396–400, doi:10.1038/nature16183, 2015.
- Korsgaard, N. J., Nuth, C., Khan, S. A., Kjeldsen, K. K., Bjørk, A. A., Schomacker, A., and Kjær, K. H.: Digital elevation model and orthophotographs of Greenland based on aerial photographs from 1978–1987, *Nature Scientific Data*, Volume 3, id. 160032 (2016)., 3, 160032, doi:10.1038/sdata.2016.32, 2016.
- 25 Krabill, W. B.: IceBridge ATM L2 Icesat Elevation, Slope, and Roughness. Version 2., doi:10.5067/CPRXXXK3F39RV., accessed: 2016-06-10, 2010, updated 2016.
- Larour, E., Seroussi, H., Morlighem, M., and Rignot, E.: Continental scale, high order, high spatial resolution, ice sheet modeling using the Ice Sheet System Model (ISSM), *Journal of Geophysical Research (Earth Surface)*, 117, F01022, doi:10.1029/2011JF002140, 2012.
- Larsen, S. H., Khan, S. A., Ahlstrøm, A. P., Hvidberg, C. S., Willis, M. J., and Andersen, S. B.: Increased mass loss and asynchronous
30 behavior of marine-terminating outlet glaciers at Upernavik Isstrøm, NW Greenland, *Journal of Geophysical Research (Earth Surface)*, 121, 241–256, doi:10.1002/2015JF003507, 2016.
- Lea, J. M., Mair, D. W. F., Nick, F. M., Rea, B. R., van As, D., Morlighem, M., Nienow, P. W., and Weidick, A.: Fluctuations of a Greenlandic tidewater glacier driven by changes in atmospheric forcing: observations and modelling of Kangiata Nunaata Sermia, 1859-present, *The Cryosphere Discussions*, 8, 2005–2041, doi:10.5194/tcd-8-2005-2014, 2014.
- 35 MacAyeal, D. R.: Large-scale ice flow over a viscous basal sediment - Theory and application to ice stream B, Antarctica, *Journal of Geophysical Research*, 94, 4071–4087, doi:10.1029/JB094iB04p04071, 1989.
- MacAyeal, D. R.: Binge/purge oscillations of the Laurentide Ice Sheet as a cause of the North Atlantic's Heinrich events, *Paleoceanography*, 8, 775–784, doi:10.1029/93PA02200, 1993.

- McConnell, J. R., Lamorey, G., Hanna, E., Mosley-Thompson, E., Bales, R. C., Belle-Oudry, D., and Kyne, J. D.: Annual net snow accumulation over southern Greenland from 1975 to 1998, *Journal of Geophysical Research: Atmospheres*, 106, 33 827–33 837, doi:10.1029/2001JD900129, 2001.
- McMillan, M., Leeson, A., Shepherd, A., Briggs, K., Armitage, T. W. K., Hogg, A., Kuipers Munneke, P., Broeke, M., Noël, B., Berg,
5 W. J., Ligtenberg, S., Horwath, M., Groh, A., Muir, A., and Gilbert, L.: A high-resolution record of Greenland mass balance, *Geophysical Research Letters*, 43, 7002–7010, doi:10.1002/2016GL069666, 2016.
- Moon, T., Joughin, I., Smith, B., Broeke, M. R., Berg, W. J., Noël, B., and Usher, M.: Distinct patterns of seasonal Greenland glacier velocity, *Geophysical Research Letters*, 41, 7209–7216, doi:10.1002/2014GL061836, 2014.
- Morlighem, M., Rignot, E., Seroussi, H., Larour, E., Ben Dhia, H., and Aubry, D.: Spatial patterns of basal drag inferred using control
10 methods from a full-Stokes and simpler models for Pine Island Glacier, West Antarctica, *Geophysical Research Letters*, 37, L14 502, doi:10.1029/2010GL043853, 2010.
- Morlighem, M., Bondzio, J., Seroussi, H., Rignot, E., Larour, E., Humbert, A., and Rebuffi, S.: Modeling of Store Gletscher’s calving dynamics, West Greenland, in response to ocean thermal forcing, *Geophysical Research Letters*, 43, 2659–2666, doi:10.1002/2016GL067695, 2016a.
- 15 Morlighem, M., Rignot, E., and Willis, J. K.: Improving Bed Topography Mapping of Greenland Glaciers Using NASA’s Oceans Melting Greenland (OMG) Data, *Oceanography*, 29, <https://doi.org/10.5670/oceanog.2016.99>, 2016b.
- Morlighem, M., Williams, C. N., Rignot, E., An, L., Bamber, J. L., Catania, G., Dowdeswell, J. A., Dorschel, B., Fenty, I., Hogan, K., Howat, I., Hubbard, A., Jakobsson, M., Jordan, T. M., Kjeldsen, K. K., Millan, R., Mayer, L., Mouginot, J., Palmer, S., Rysgaard, S., Seroussi, H., Slabon, P., Straneo, F., Weinrebe, W., Wood, M., and Zinglensen, B.: BedMachine v3: Complete bed topography and ocean bathymetry
20 mapping of Greenland from multi-beam echo sounding combined with mass conservation, doi:10.1002/2017GL074954, 2017.
- Motyka, R. J., Truffer, M., Fahnestock, M., Mortensen, J., Rysgaard, S., and Howat, I. M.: Submarine melting of the 1985 Jakobshavn Isbrae floating tongue and the triggering of the current retreat, *Journal of Geophysical Research*, 116, 1–17, doi:10.1029/2009JF001632, 2011.
- Nagler, T., Forsberg, R., Marcus, E., and Hauglund, K.: Product User Guide (PUG) for the Greenland Ice Sheet cci project of ESA’s Climate Change Initiative, version 2.1, <http://www.esa-icesheets-greenland-cci.org/>, 2017.
- 25 Nick, F. M., Vieli, A., Howat, I. M., and Joughin, I.: Large-scale changes in Greenland outlet glacier dynamics triggered at the terminus, *Nature Geoscience*, 2, 110–114, doi:10.1038/ngeo394, 2009.
- Nick, F. M., van der Veen, C. J., Vieli, A., and Benn, D. I.: A physically based calving model applied to marine outlet glaciers and implications for the glacier dynamics, *Journal of Glaciology*, 56, 781–794, doi:10.3189/002214310794457344, 2010.
- Nick, F. M., Vieli, A., Andersen, M. L., Joughin, I., Payne, A., Edwards, T. L., Pattyn, F., and van de Wal, R. S. W.: Future sea-level rise
30 from Greenland’s main outlet glaciers in a warming climate, *nature*, 497, 235–238, doi:10.1038/nature12068, 2013.
- Noh, M.-J. and Howat, I. M.: Automated stereo-photogrammetric DEM generation at high latitudes: Surface Extraction with TIN-based Search-space Minimization (SETSM) validation and demonstration over glaciated regions, *GIScience & Remote Sensing*, 52, 198–217, doi:10.1080/15481603.2015.1008621, 2015.
- O’Leary, M. and Christoffersen, P.: Calving on tidewater glaciers amplified by submarine frontal melting, *Cryosphere*, 7, 119–128,
35 doi:10.5194/tc-7-119-2013, 2013.
- OMG Mission.: Bathymetry (sea floor depth) data from the ship-based bathymetry survey. Ver. 0.1, doi:10.5067/OMGEV-BTYSS, dataset accessed: 2016-06-10, 2016.

- Podrasky, D., Truffer, M., Fahnestock, M., Amundson, J., Cassotto, R., and Joughin, I.: Outlet glacier response to forcing over hourly to interannual timescales, Jakobshavn Isbræ, Greenland, *Journal of Glaciology*, 58, 1212–1226, doi:10.3189/2012JoG12J065, 2012.
- Pritchard, H. D., Arthern, R. J., Vaughan, D. G., and Edwards, L. A.: Extensive dynamic thinning on the margins of the Greenland and Antarctic ice sheets, *nature*, 461, 971–975, doi:10.1038/nature08471, 2009.
- 5 Rignot, E. and Mouginot, J.: Ice flow in Greenland for the International Polar Year 2008–2009, *Geophysical Research Letters*, 39, L11 501, doi:10.1029/2012GL051634, 2012.
- Rignot, E., Velicogna, I., van den Broeke, M. R., Monaghan, A., and Lenaerts, J. T. M.: Acceleration of the contribution of the Greenland and Antarctic ice sheets to sea level rise, *Geophysical Research Letters*, 38, L05 503, doi:10.1029/2011GL046583, 2011.
- Rignot, E., Fenty, I., Xu, Y., Cai, C., Velicogna, I., Ó Cofaigh, C., Dowdeswell, J. A., Weinrebe, W., Catania, G. A., and Duncan, D.:
10 Bathymetry data reveal glaciers vulnerable to ice-ocean interaction in Uummannaq and Vaigat glacial fjords, west Greenland, *Geophysical Research Letters*, 2014, 1–8, doi:10.1002/2016GL067832.Received, 2016.
- Rosenau, R., Schwalbe, E., Maas, H.-G., Baessler, M., and Dietrich, R.: Grounding line migration and high-resolution calving dynamics of Jakobshavn Isbræ, West Greenland, *Journal of Geophysical Research (Earth Surface)*, 118, 382–395, doi:10.1029/2012JF002515, 2013.
- Schlegel, N.-J., Wiese, D. N., Larour, E. Y., Watkins, M. M., Box, J. E., Fettweis, X., and van den Broeke, M. R.: Application of GRACE
15 to the assessment of model-based estimates of monthly Greenland Ice Sheet mass balance (2003–2012), *The Cryosphere*, 10, 1965–1989, doi:10.5194/tc-10-1965-2016, 2016.
- Seroussi, H., Morlighem, M., Larour, E., Rignot, E., and Khazendar, A.: Hydrostatic grounding line parameterization in ice sheet models, *The Cryosphere Discussions*, 8, 3335–3365, doi:10.5194/tcd-8-3335-2014, 2014.
- Shepherd, A. and Nowicki, S.: Improvements in ice-sheet sea-level projections, *Nature Climate Change*, 7, 672–674,
20 doi:10.1038/nclimate3400, 2017.
- Thomas, R. and Studinger, M. S.: Pre-IceBridge ATM L2 Icessn Elevation, Slope, and Roughness, Version 1., doi:10.5067/6C6WA3R918HJ, accessed: 2016-06-10, 2010.
- Todd, J. and Christoffersen, P.: Are seasonal calving dynamics forced by buttressing from ice mélange or undercutting by melting? Outcomes from full-Stokes simulations of Store Glacier, West Greenland, *The Cryosphere*, 8, 2353–2365, doi:10.5194/tc-8-2353-2014, 2014.
- 25 van As, D., Fausto, R. S., Cappelen, J., Van de Wal, R. S. W., Braithwaite, R. J., Machguth, H., and PROMICE project team: Placing Greenland ice sheet ablation measurements in a multi-decadal context, *Geol. Surv. Denmark Greenland Bull.*, 35, 71–74, 2016.
- van den Broeke, M., Bamber, J., Ettema, J., Rignot, E., Schrama, E., van de Berg, W. J., van Meijgaard, E., Velicogna, I., and Wouters, B.: Partitioning Recent Greenland Mass Loss, *Science*, 326, 984, doi:10.1126/science.1178176, 2009.
- Velicogna, I., Sutterley, T. C., and van den Broeke, M. R.: Regional acceleration in ice mass loss from Greenland and Antarctica using
30 GRACE time-variable gravity data, *Geophysical Research Letters*, 41, 8130–8137, doi:10.1002/2014GL061052, 2014.
- Watkins, M. M., Wiese, D. N., Yuan, D.-N., Boening, C., and Landerer, F. W.: Improved methods for observing Earth’s time variable mass distribution with GRACE using spherical cap mascons, *Journal of Geophysical Research: Solid Earth*, 120, 2648–2671, doi:10.1002/2014JB011547, 2015.
- Weidick, A.: Frontal variations at Upernaviks Isstrøm in the last 100 years, *Meddelser fra Dansk Geologisk Forening*, 14, 52–60, 1958.
- 35 Wiese, D. N., Yuan, D.-N., Boening, C., Landerer, F. W., and Watkins, M. M.: JPL GRACE Mascon Ocean, Ice, and Hydrology Equivalent Water Height RL05M.1 CRI Filtered, Ver. 21, doi:10.5067/TEMSC-OLCR5, dataset accessed: 2015, 2015.

Supplement of

Simulating ice thickness and velocity evolution of Upernavik Isstrøm 1849-2012 by forcing prescribed terminus positions in ISSM

5

Konstanze Haubner et al.

Correspondence to: Konstanze Haubner (khu@geus.dk)

Model initialisation

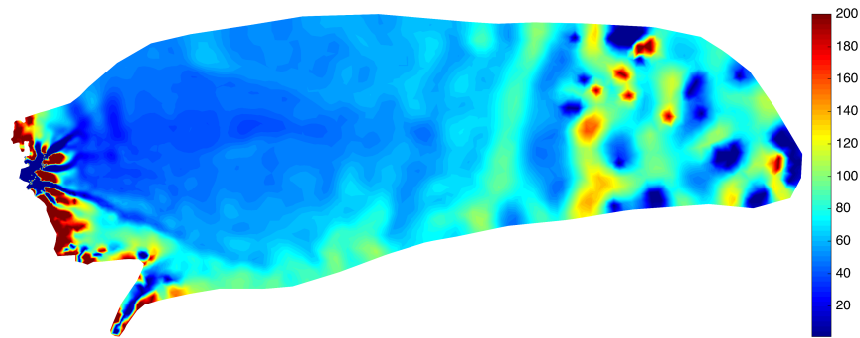


Figure 1. Inverted basal friction coefficient

10

Simulation comparison: 1849 to 2012

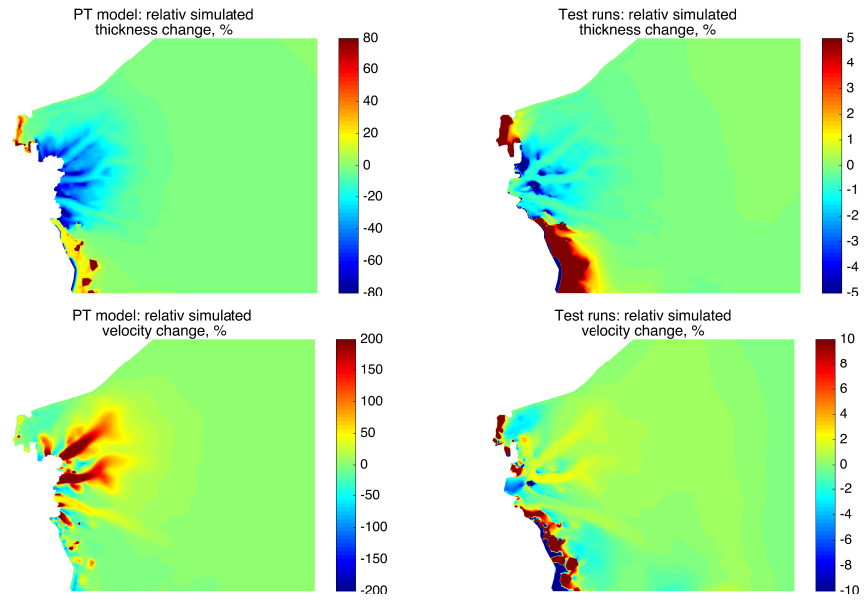


Figure 2. Simulated ice thickness and velocity changes 2012–1849.

Ice thickness comparison: simulation - observations

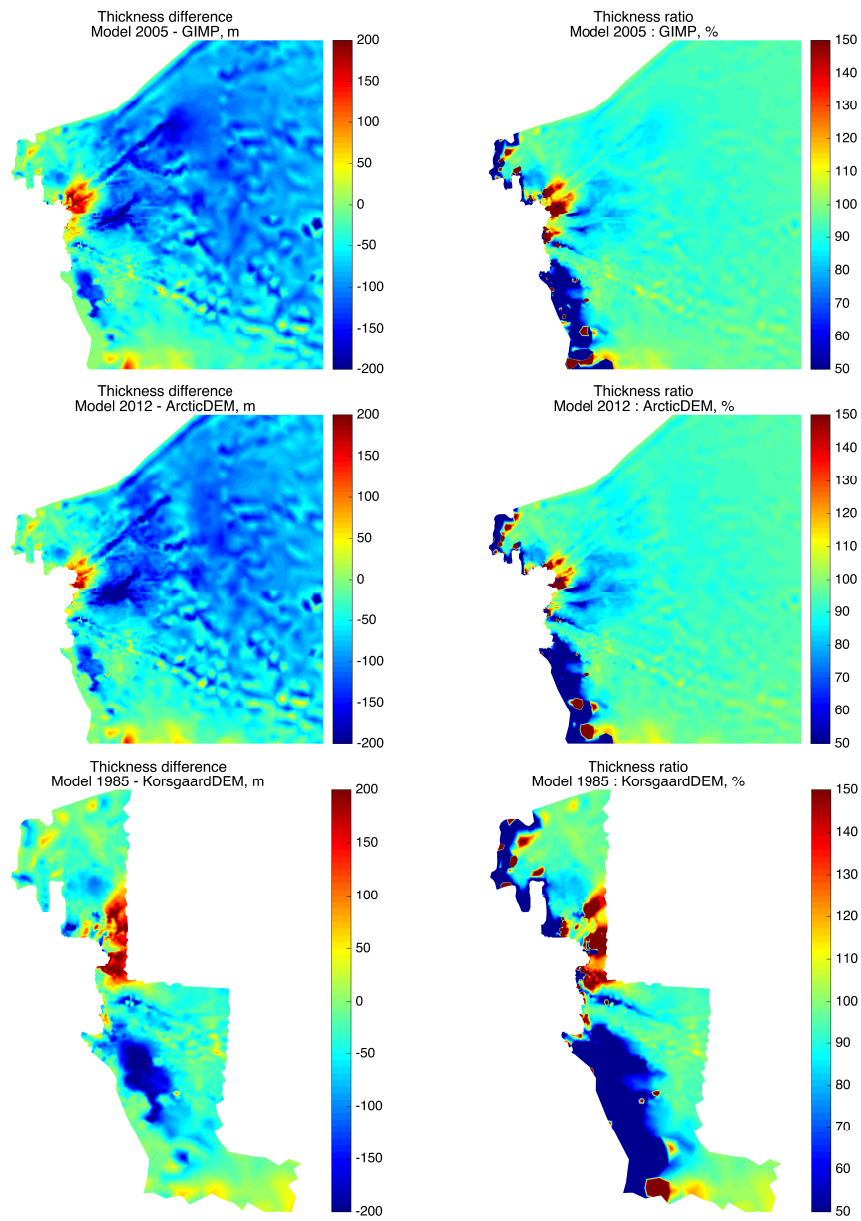


Figure 3. Comparison of simulated and observed ice thickness in 1985 (Korsgaard DEM), 2005 (GIMP) and 2012 (ArcticDEM).

Surface velocity comparison: simulation - observations

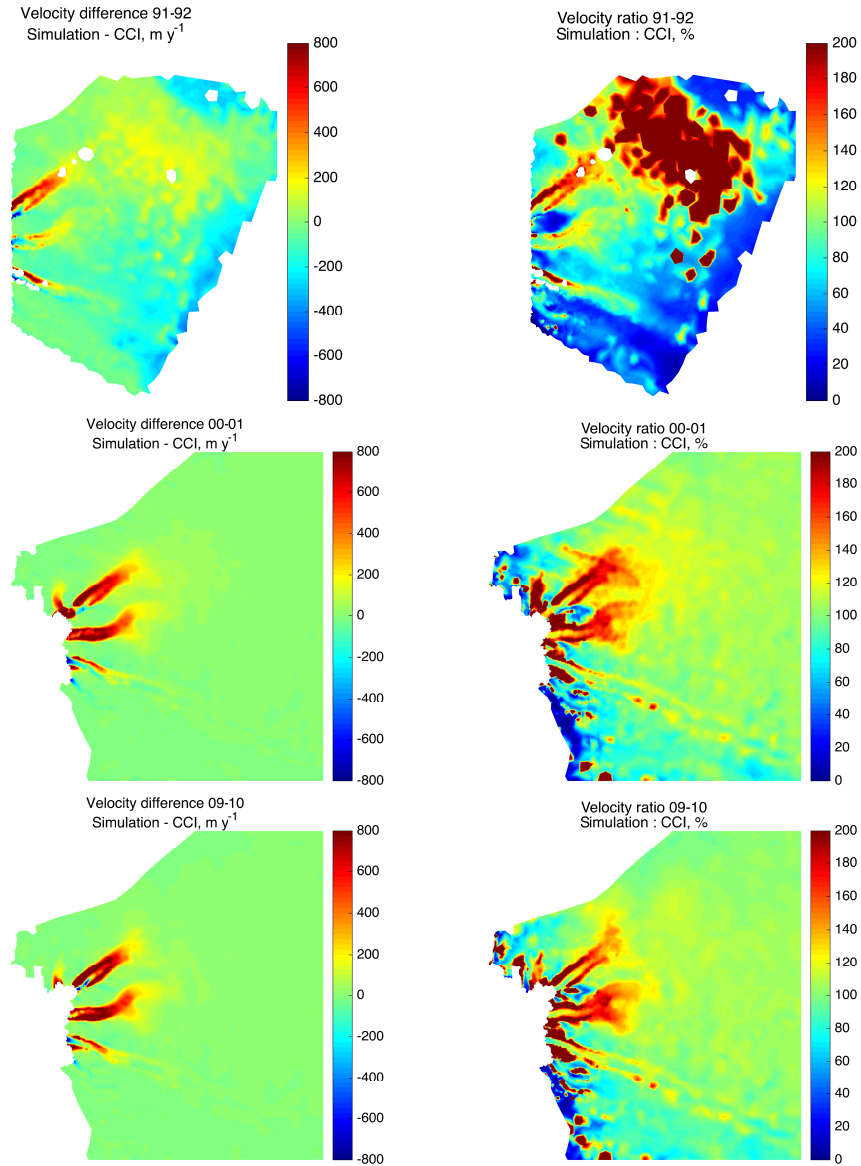


Figure 4. Comparison of simulated and observed ice surface velocity in 1991/1992 (CCI, Envisat), 2000/2001 (MEaSURES) and 2009/2010 (MEaSURES), representing begin, middle and end of observation time.

Mass change comparison - GRACE

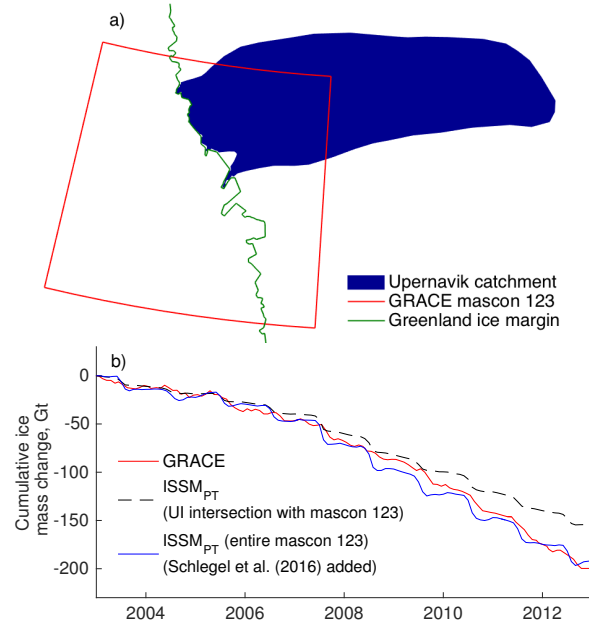


Figure 5. (a) GRACE area overview. UI catchment and model domain (blue polygon), present Greenland ice margin (green line) and the GRACE mascon (red line). (b) Mass change comparison between 2003 and 2012. GRACE (red), simulated mass loss of the intersection area of mascon 123 and model domain (dashed line) and a simulated mass loss (sum of ISSM_{PT} simulated mass loss in mascon 123 and the ISSM SSA model output of Schlegel et al. (2016) to cover the entire domain) (blue line).

References

Schlegel, N.-J., Wiese, D. N., Larour, E. Y., Watkins, M. M., Box, J. E., Fettweis, X., and van den Broeke, M. R.: Application of GRACE to the assessment of model-based estimates of monthly Greenland Ice Sheet mass balance (2003-2012), *The Cryosphere*, 10, 1965–1989, doi:10.5194/tc-10-1965-2016, 2016.